Stimuli-Responsive Double Hydrophilic Block Copolymer Micelles with Switchable Catalytic Activity

Zhishen Ge,[†] Dang Xie,[‡] Daoyong Chen,[‡] Xiaoze Jiang,[†] Yanfeng Zhang,[†] Hewen Liu,[†] and Shiyong Liu[†,*]

Department of Polymer Science and Engineering, Hefei National Laboratory for Physical Sciences at the Microscale, University of Science and Technology of China, Hefei, Anhui 230026, China, and Department of Macromolecular Science, Fudan University, Shanghai 200433, China

Received March 6, 2007; Revised Manuscript Received March 18, 2007

ABSTRACT: Double hydrophilic block copolymers, poly(*N*-isopropylacrylamide)-*b*-poly(*N*-vinylimidazole) (PNIPAM-*b*-PVim), were successfully prepared with good control via reversible addition−fragmentation chain transfer (RAFT) using PNIPAM-based macromolecular xanthate agents (i.e., MADIX, macromolecular design via the interchange of xanthates). This represents the first preparation of well-defined block copolymers based on PVim, which has been well-known to be able to catalyze esterolysis reactions. The imidazole-containing diblock copolymers molecularly dissolve at low temperatures in water. Above the phase transition temperatures of PNIPAM or in a proper mixture of methanol/water (cononsolvency), the PNIPAM block becomes hydrophobic and stable micelles form with a dense core consisting of a hydrophobic PNIPAM block and a polar PVim shell. The catalytic activities of $PNIPAM_{44}$-*b*-$PVim_{51}$ and $PNIPAM_{44}$-*b*-$PVim_{21}$ toward the hydrolysis of *p*-nitrophenyl acetate (NPA) at different temperatures or methanol/water compositions were then determined using a stopped-flow apparatus and compared to that of PVim homopolymer. The Arrhenius plot for the PVim-based diblock copolymers exhibited a pronounced upward curvature above the critical micellization temperature (cmt). Moreover, in the methanol/water mixture, the catalytic activities of PNIPAM-*b*-PVim diblock copolymers evolved discontinuously as a function of solvent composition and exhibited a maximum in the range of volume fraction of methanol, $\varphi_{methanol}$, between 0.3 and 0.5, corresponding to the solvent composition range where cononsolvency-induced micellization took place. We thus observed for the first time that double hydrophilic block copolymer micelles of PNIPAM-*b*-PVim can serve as self-catalyzing nanoreactors. Most importantly, the catalytic activities can be well-tuned with external temperature or solvent compositions.

Introduction

In aqueous solution amphiphilic block copolymers can self-assemble into micelles with hydrophobic block as the core and hydrophilic block as the shell.[1−6] Among them, double hydrophilic block copolymers (DHBCs) represent a special type of example, exhibiting "schizophrenic" micellization behavior due to that the water solubility of one or both blocks can be altered.[7−22] They can self-assemble and form micellar or "reverse" micellar structures in water if external conditions such as temperature, pH, and ionic strengths are properly tuned. The past studies on DHBCs mainly focused on the determination of the aggregation numbers, critical micellization concentration (cmc), and the size and shape of various aggregates. Much less has been exploited on their application as water-soluble catalysts, although this research area has long been a subject of considerable interest, inspired by the investigation of the mechanism of highly selective and efficient enzyme catalysis.[23,24]

On the other hand, imidazole-containing homopolymers,[25−27] random copolymers,[23,24,28] and polymer networks[29,30] have been extensively explored as water-soluble catalysts. Poly(*N*-vinylimidazole) (PVim) is well-known to be a selective catalyst for esterolysis via the formation of catalyst-substrate complex.[26] By copolymerizing with hydrophobic or charged monomers with *N*-vinylimidazole (Vim), the adsorption of substrates at the chains of polymer catalyst can be further improved via hydrophobic association or electrostatic interactions.[24,31]

In terms of their practical applications, polymer catalysts with tunable or switchable catalytic activities would be highly desirable. Several attempts were made toward this task. Wang et al.[29] synthesized polymer gel consisting of *N*-isopropylacrylamide (NIPAM) and 4(5)-vinylimidazole, with the former being the major component. They found that the catalytic activity of the gel for esterolysis can be switched on or of by adjusting the solvent compositions (water/ethanol), utilizing the fact that poly(*N*-isopropylacrylamide) (PNIPAM) undergoes a phase transition in the mixed solvent within a specific range.[32] In the solvent composition range where the polymer gel collapsed, prominent enhancement of the catalytic activity was observed, suggesting that the hydrophobic PNIPAM network increased affinity for the substrate, thus enhancing the catalytic activities. It is noteworthy that the macrosized gel catalysts may be plagued with transport limitations due to its low interfacial area.

PNIPAM is also well-known as a thermoresponsive polymer, exhibiting a lower critical solution temperature (LCST) at ∼ 32 °C.[32] Khokhlov et al.[23,33] further improved the idea of tuning the catalytic activity of imidazole-containing polymers. They synthesized PNIPAM-*co*-PVim random copolymers. At temperatures above the LCST, the polymer chains exhibit a coil-to-globule transition with subsequent formation of globular aggregates of submicrometer sizes, and enhanced catalytic activity was observed.[23] The aggregates can be considered as microheterogeneous nanoreactors and quite comparable to that of micellar catalysis in the presence of small molecule surfactants by concentrating the substrates inside the hydrophobic core.[24,34] However, at even higher temperatures (>45 °C), the aggregates were not stable probably due to the random sequence

* To whom correspondence should be addressed. E-mail: sliu@ustc.edu.cn.
[†] University of Science and Technology of China.
[‡] Fudan University.

10.1021/ma070550i CCC: $37.00
Published on Web 04/13/2007

of two different types of monomers, and decreased catalytic activity was observed.

Considering that previously reported imidazole-containing polymeric catalysts did not possess well-defined chemical structures (uncertain monomer sequences and broad molecular weight distributions), Patrickios et al.[30,35] synthesized poly(2-(1-imidazolyl)ethyl methacrylate)-*b*-poly(2-(dimethylamino)-ethyl methacrylate (PImEMA-*b*-PDMAEMA). They initially speculated that the block copolymer will assemble into PImEMA-core micelles, and the selective partitioning of hydrophobic substrate inside the imidazole core will accelerate the reactions. However, although possessing much lower water solubility than PVim, the hydrophobicity of PImEMA block is not sufficient for extensive micellization, they did not observe enhanced catalytic activity of the block copolymers compared to the corresponding random copolymers.[30] It should be noted that the PDMAEMA block, being a weak base and nucleophile, may also exhibit catalytic activities.

In light of these considerations, herein, we explore the idea of controlling the catalytic activity of hydrolysis by employing stimuli-responsive double hydrophilic diblock copolymers, PNIPAM-*b*-PVim. The diblock copolymer can molecularly dissolve at low temperatures in water. At elevated temperatures or in a proper mixture of methanol/water, PNIPAM block became hydrophobic and stable micelles with a dense core consisting of hydrophobic PNIPAM block and a polar shell formed by PVim will form. During hydrolytic catalysis, hydrophobic substrate will concentrate within the hydrophobic core of micelles and catalyzed by outer PVim shell. We may observe enhanced reaction rate employing the double hydrophilic block copolymer micelles as catalysts. Most importantly, as the micelle formation can be switched on or off by changing external temperatures or solvent compositions, we should be able to finely tune the catalytic activities. Thus, this type of water-soluble catalysts can combine the advantages of micro-heterogeneous nanoreactors, micellar catalysis, and tunable catalytic activities.

To the best of our knowledge, the preparation of PVim homopolymer with narrow polydispersity and well-defined PVim-based block copolymers has never been reported. Although the past 10 years has evidenced tremendous progress in controlled/living free radical polymerizations, such as nitroxide-mediated polymerization (NMP),[36] reversible addition−fragmentation chain transfer (RAFT),[37,38] and atom transfer radical polymerization (ATRP),[39,40] the controlled polymerization of Vim is still challenging. Vim monomer contains an imidazole group, and the nitrogen is directly attached to the vinyl group. Thus, the vinyl group is not conjugated with the carbonyl group unlike acrylamides.[41] A big advantage toward the synthesis of well-defined PVim homopolymer and block copolymers is that monomers with similar structures, such as *N*-vinyl-2-pyrrolidinone[42] or *N*-vinylformamide,[43] have recently been polymerized in a controlled manner via RAFT or MADIX (macromolecular design via the interchange of xanthates) using xanthate as chain transfer agents (CTAs).[44,45]

In this communication, we conducted the RAFT/MADIX polymerization of NIPAM using [1-(*o*-ethylxanthyl)ethyl]benzene (**1**) as the CTA. We then investigated the "controlled" free radical polymerization of Vim in the presence of PNIPAM-based macro-CTA, and synthesized PNIPAM-*b*-PVim block copolymers. The micellization behavior of PNIPAM-*b*-PVim in aqueous solution and water/methanol solvent mixtures was then characterized in detail by laser light scattering (LLS) and transmission electron microscopy (TEM). Moreover, the block copolymer aggregates were tested as hydrolytic catalysts with tunable or switchable activities for *p*-nitrophenyl acetate (NPA), the reaction kinetics of which was accurately monitored by the stopped-flow apparatus.

Experimental Section

Materials. *N*-Isopropylacrylamide (NIPAM) (97%, Tokyo Kasei Kagyo Co.) was purified by recrystallization in a benzene/*n*-hexane mixture. 2,2′-azobis(isobutyronitrile) (AIBN) was recrystallized from 95% ethanol. *p*-Nitrophenyl acetate (NPA, Fluka) was recrystallized from 2-propanol. *N*-vinylimidazole (Vim, Fluka) was dried over CaH_2 and distilled under reduced pressure. [1-(*O*-ethylxanthyl)ethyl]benzene (**1**) was prepared according to the literature procedures.[42] Other chemicals were purchased from Shanghai Chemical Reagent Co. and used as received.

Polymer Synthesis. A glass ampule was charged with **1** (0.1 g, 0.44 mmol), AIBN (9.0 mg, 0.055 mmol), NIPAM (3.5 g, 31 mmol), and 1,4-dioxane (7 mL); it was then degassed by three freeze−thaw cycles and sealed under vacuum. The polymerization was carried out at 80 °C for 12 h. The mixture was precipitated into anhydrous diethyl ether three times. The product was collected by filtration and then dried in a vacuum oven at room temperature. Slightly yellowish solids were obtained with a yield of 59.2%. GPC analysis in DMF revealed a monomodal peak with $M_n \sim 5400$, and a polydispersity, M_w/M_n, of 1.14. The degree of polymerization (DP) of PNIPAM was determined to be 44 by ^{1}H NMR.

The above obtained PNIPAM was used as the macro-CTA for the synthesis of PNIPAM-*b*-PVim. A typical procedure was as follows. A mixture of PNIPAM macro-CTA (0.54 g, 0.1 mmol), AIBN (2.0 mg, 0.0125 mmol), and Vim (1.03 g, 11 mmol) was mixed in DMF (4 mL), it was then degassed by three freeze−thaw cycles and sealed under vacuum. The polymerization was carried out at 80 °C for 24 h. The mixture was precipitated into anhydrous diethyl ether twice. The product was collected by filtration and then dried in a vacuum oven at room temperature. GPC analysis in DMF revealed a monomodal peak with $M_n \sim 11\,090$, and $M_w/M_n \sim 1.21$.The degree of polymerization (DP) of the PVim block was determined to be 51 by ^{1}H NMR. In this study, two imidazole-containing diblock copolymers, $PNIPAM_{44}$-*b*-$PVim_{21}$ and $PNIPAM_{44}$-*b*-$PVim_{51}$, were prepared.

To monitor kinetics of the polymerization of Vim using PNIPAM macroRAFT agent, a mixture of PNIPAM-based macro-CTA (1.62 g, 0.3 mmol), AIBN (6.2 mg, 0.0375 mmol), and Vim (2.82 g, 30 mmol) was degassed by three freeze−vacuum−thaw cycles. The solution was evenly charged into six glass tubes, and the tubes were flame-sealed under vacuum. The tubes were immersed into thermostatic oil bath at 80 °C. At timed intervals, the polymerization tubes were taken out and quenched into liquid nitrogen to terminate the reaction. The solution mixture was then subjected to ^{1}H NMR and DMF GPC analysis directly.

For the observation of possible enhancement of reaction rate using the block copolymer micelles as catalysts, PVim homopolymer was also synthesized as a control via the RAFT/MADIX process using **1** as the CTA. The degree of polymerization of PVim homopolymer was determined to be 65 by ^{1}H NMR. GPC analysis revealed a monomodal peak with an $M_n \sim 8400$ and an $M_w/M_n \sim 1.23$.

Characterization. Nuclear Magnetic Resonance (NMR) Spectroscopy. All ^{1}H NMR spectra were recorded using a Bruker 300 MHz spectrometer in $CDCl_3$ or D_2O.

Gel Permeation Chromatography (GPC). Molecular weights and molecular weight distributions were determined by GPC using a series of three linear Styragel columns (HT3, HT4, and HT5) and an oven temperature of 50 °C. Waters 1515 pump and Waters 2414 differential refractive index detector (set at 35 °C) was used. The eluent was DMF at a flow rate of 1.0 mL/min. The number-average (M_n) and molecular weight distribution (M_w/M_n) for the sample polymers were calibrated with standard poly(ethylene oxide) samples.

Scheme 1. (a) Overall Reaction in the RAFT/MADIX Polymerization and (b) Schematic Illustration for the Preparation of PNIPAM-*b*-PVim Diblock Copolymers

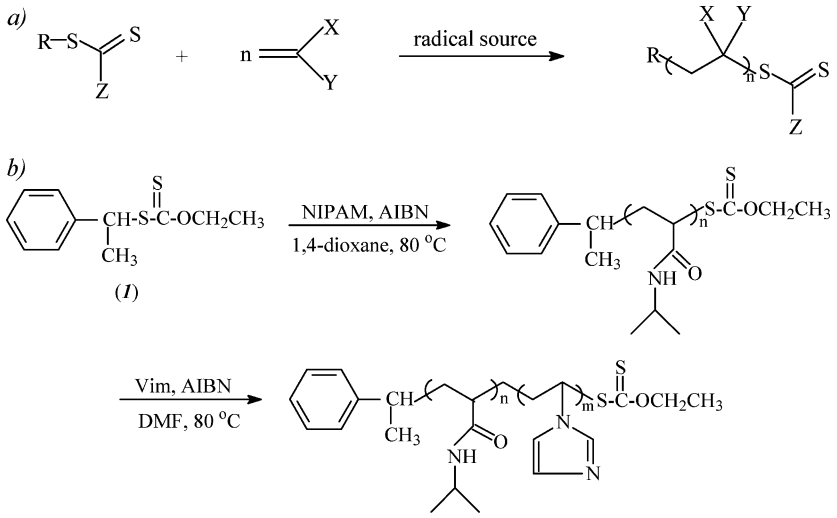

TEM observations were conducted on a Hitachi H-800 electron microscope at an acceleration voltage of 200 kV. The sample for TEM observations was prepared by placing a light drop of solution on copper grids coated with thin films of Formvar and carbon successively.

Laser Light Scattering (LLS). A commercial spectrometer (ALV/DLS/SLS-5022F) equipped with a multitau digital time correlator (ALV5000) and a cylindrical 22 mW UNIPHASE He−Ne laser (λ_0 = 632 nm) as the light source was employed for dynamic and static LLS measurements. In static LLS, we can obtain the weight-average molar mass (M_w) and the *z*-average root-mean square radius of gyration ($\langle R_g^2 \rangle^{1/2}$ or written as $\langle R_g \rangle$) of polymer chains or aggregates in a dilute solution from the angular dependence of the excess absolute scattering intensity, known as Rayleigh ratio $R_{vv}(q)$. The specific refractive index increments (d*n*/d*C*) of micellar solution of PNIPAM$_{44}$-*b*-PVim$_{21}$ and PNIPAM$_{44}$-*b*-PVim$_{51}$ at 40 °C were determined to be 0.183 and 0.191 mL/g, respectively, by a precise differential refractometer at the same wavelength of 632 nm as in LLS measurements. For the determination of the molar masses of block copolymer micelles, only one polymer concentration (5×10^{-4} g/mL) was used. Thus, the obtained M_w should only be considered as apparent values, denoted as $M_{w,app}$.

Stopped-Flow Kinetic Measurements. Stopped-flow studies were carried out using a Bio-Logic SFM300/S stopped-flow instrument. The SFM-3/S is a three-syringe (10 mL) instrument in which all step-motor-driven syringes (S1, S2, S3) can be operated independently to carry out single- or double-mixing. The SFM-300/S stopped-flow device is attached to the MOS-250 spectrometer. The kinetic data were fitted using the program Biokine (Bio-Logic). For the absorbance detection, both the excitation and emission wavelengths were adjusted to 402 nm with 5 nm slits. Using FC-08 or FC-15 flow cells, the typical dead times are 1.1 and 2.6 ms, respectively. The applied voltage to the photomultiplier was fixed at 284 V.

Kinetic measurements at different temperatures were performed at final (after mixing) Vim and NPA concentrations of 2 mM in water/2-propanol (IPA, 10 vol %).[23] The solutions were buffered at pH 7.4 with 2 mM KH_2PO_4/Na_2HPO_4). For the catalytic reactions conducted in the methanol/water mixture, the final concentrations of Vim and NPA were also fixed at 2 mM after stopped-flow mixing the polymer catalysts in buffer (0.05 M Tris·HCl, pH 7.4) and NPA in methanol.[29] Temperatures were maintained at 293 K. The progress of catalytic reaction was monitored by tracing the rate of absorbance increase at 402 nm due to the release of *p*-nitrophenol in its ionized form.

Results and Discussion

Polymer Synthesis. In the RAFT/MADIX polymerizations (see Scheme 1a), the Z group mainly influences the rate of addition of radicals to the C═S double bond.[41] The variation of Z group can also lead to changes in the stability/reactivity of the macroradical intermediates. It has been well-established that dithioesters (e.g., with $Z = CH_3$ or Ph and R = cumyl) are particularly efficient in the RAFT polymerization of styrene and alkyl acrylate to produce polymers with low polydispersity and predetermined molecular weights.[37,38,41] Another particular type of RAFT polymerization, macromolecular design via the interchange of xanthates (MADIX), employs xanthates (i.e., Z = *O*-alkyl) as chain transfer agents (CTAs).[41,44,45] The conjugation of the C═S double bond with the electron doublets of the oxygen atom results in a slow exchange of the dithiocarbonate moieties among propagating and dormant polymeric chains.

In the Vim monomer, the vinyl group is not conjugated with the carbonyl group. For a CTA to react rapidly with the propagating radicals, the polymerization intermediates need to be less stable than in the polymerizations of most other monomers.[41] Thus, although most conventional thiocarbonylthio compounds retard considerably the polymerization of nonconjugated monomers, xanthates (MADIX technique) allow reasonably good control of the polymerization of monomers such as *N*-vinylpyrrolidone,[42] *N*-vinylformamide,[43] and vinyl acetate.[44] Typical polydispersity were ∼1.2−1.4. As Vim monomers are structurally similar to *N*-vinylpyrrolidone and *N*-vinylformamide, we chose the MADIX technique to prepare PVim-based block copolymers in this study.

One basic requirement for the preparation of a well-defined diblock copolymer with narrow polydispersity is that the first formed polymeric thiocarbonylthiol compound should have a high chain transfer constants compared to that of the second monomer; otherwise, incomplete reinitiation will take place.[41] This requires that the leaving ability of the first block is comparable to, or favorably greater than, that of the propagating radical of the second block under the reaction conditions (i.e., higher stability of the reinitiating radical). Scheme 1b shows the reaction scheme for the preparation of PNIPAM-*b*-PVim. First, *O*-ethyl xanthate was used to polymerize NIPAM, the obtained polymer was then employed as the polymeric macro-CTA for the polymerization of Vim to obtain the target diblock copolymers.

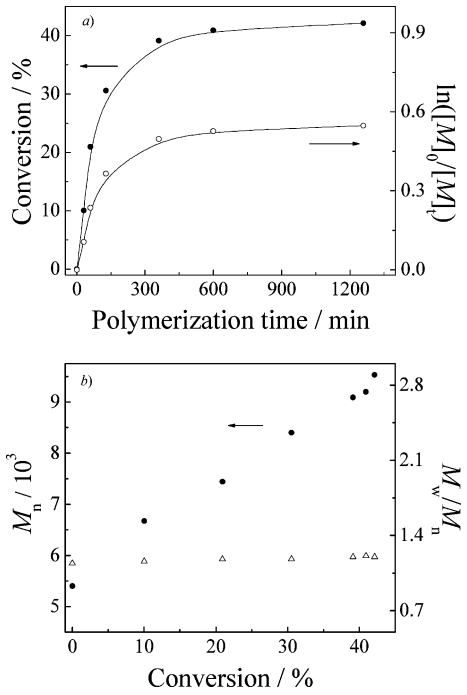

Figure 1. (a) Time−conversion and the first-order kinetic plots for the polymerization of Vim in the presence of PNIPAM macro-CTA at 80 °C under vacuum. (b) Dependence of M_n and M_w/M_n on the monomer conversions during the polymerization of Vim in the presence of PNIPAM macro-CTA at 80 °C.

The RAFT polymerization of NIPAM monomer, affording PNIPAM macro-CTA, has been well-established and quite straightforward.[41,46,47] Using xanthate **1** as the CTA, PNIPAM terminated with a xanthate moiety (Scheme 1b) with relatively narrow polydispersity (M_n = 5400 and M_w/M_n = 1.14) was obtained and employed as macro-CTA for the polymerization of Vim.

Figure 1a shows the time−conversion and the first-order kinetic plots for the polymerization of Vim in the presence of PNIPAM macro-CTA and AIBN at 80 °C. For the kinetic measurements, the polymerization tubes were taken out at timed intervals from the oil bath and the reaction mixture was directly subjected to ^{1}H NMR and GPC analysis. The pseudo-first-order kinetic plot is consistent with a "living" polymerization mechanism over the first 150 min, indicating that the concentration of active propagating radical species remains almost constant during the early stages of polymerization. Beyond 150 min, downward curvature is clearly evident, suggesting a decreasing concentration of propagating radicals.

Figure 1b plots M_n and M_w/M_n of the polymers obtained by RAFT/MADIX polymerization of Vim in the presence of PNIPAM macro-CTA as a function of the monomer conversions. The M_n, M_w/M_n values and the monomer conversions were determined from DMF GPC and ^{1}H NMR analyses, respectively. The increase of M_n with conversion is practically linear, and the M_w/M_n values keep in a somewhat narrow range of 1.15−1.25, which is almost independent of the monomer conversions. These observations indicate that the polymerization is reasonably well controlled.

Figure 2 shows the DMF GPC traces of PNIPAM macro-CTA and the resulting PNIPAM-*b*-PVim diblock copolymers. All the GPC elution profiles are unimodal and the molecular weight distributions are relatively narrow. Compared to the PNIPAM macro-RAFT agent, all the diblock copolymers eluted at higher molecular weights and a clear shift can be observed. The absence of any shoulder at the low molecular weight side

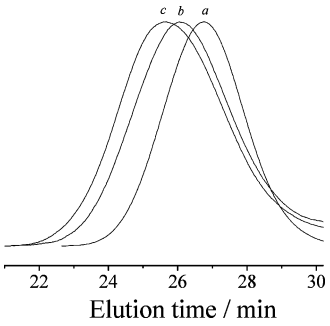

Figure 2. DMF GPC traces of (a) $PNIPAM_{44}$ (M_n = 5,400, M_w/M_n = 1.14), (b) $PNIPAM_{44}$-*b*-$PVim_{21}$ (M_n = 8,800, M_w/M_n = 1.18), and (c) $PNIPAM_{44}$-*b*-$PVim_{51}$ (M_n = 11,090, M_w/M_n = 1.21).

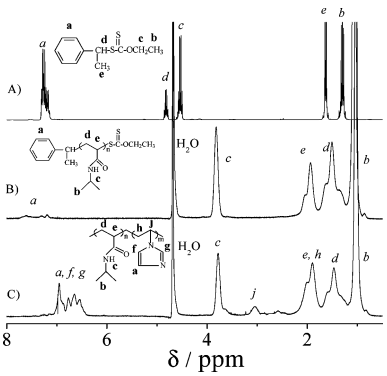

Figure 3. ^{1}H NMR spectra recorded for (A) xanthate agent **1** in $CDCl_3$, (B) $PNIPAM_{44}$ macro-CTA agent in D_2O at 20 °C, and (C) $PNIPAM_{44}$-*b*-$PVim_{51}$ in D_2O at 20 °C.

indicates that PNIPAM macro-CTA is quite efficient in mediating the polymerization of the less active monomer, Vim. However, the M_n values determined by GPC can only be considered as apparent values mainly because PEO, an uncharged polymer with no bulky side groups, was used as GPC calibration standards. The actual DP of the PVim block was determined by ^{1}H NMR.

Figure 3 shows the ^{1}H NMR spectra recorded for **1**, PNIPAM macro-CTA, and $PNIPAM_{44}$-*b*-$PVim_{51}$ in D_2O. The resonances of protons in the phenyl group and −NH−C*H*− occur at 7.2−7.7 and 3.7 −3.9 ppm, respectively (Figure 3b). From the relative intensities of these signals, the DP of PNIPAM macro-CTA can be calculated as 44. The signals in the range of 6.5−7.2 ppm are attributed to the protons of imidazole group. The resonance peaks at 1.2 and 3.7−3.9 ppm are attributed to the methyl and methine protons in the pendent isopropyl group of NIPAM monomer units, respectively. Thus, the DP of PVim block can be calculated. Two imidazole-containing diblock copolymers, $PNIPAM_{44}$-*b*-$PVim_{21}$ and $PNIPAM_{44}$-*b*-$PVim_{51}$, were prepared and used in subsequent studies. To the best of our knowledge, the preparation of PVim-based double hydrophilic block copolymers has never been reported before, thus, the detailed characterization of their stimuli-responsive micellization behavior is necessary prior to their catalytic activity studies.

Stimuli-Responsive Micellization of PNIPAM-*b*-PVim. PNIPAM homopolymer undergoes a coil-to-globule phase transition in dilute aqueous solutions at its LCST of about 32 °C.[32] At room temperature, PNIPAM can be unimolecularly dissolved in water and methanol, respectively, but not for a proper mixture of them.[48−50] This is called cononsolvency and has been extensively studied.[51] The equilibrium structures of single PNIPAM chain in extremely diluted aqueous solutions as a function of methanol/water composition have been well

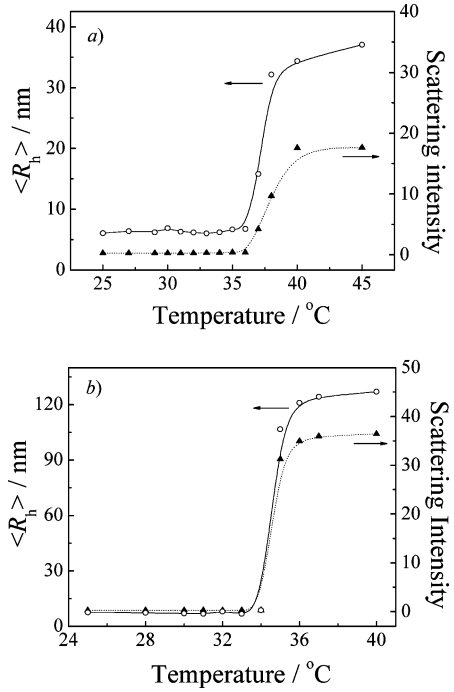

Figure 4. Temperature dependence of average hydrodynamic radius, $\langle R_h \rangle$, and scattering intensities for (a) PNIPAM$_{44}$-*b*-PVim$_{51}$ and (b) PNIPAM$_{44}$-*b*-PVim$_{21}$ in aqueous solution at a concentration of 5×10^{-4} g/mL.

characterized by Wu et al.,[52] which exhibits a reentrant coil-to-globule-to-coil transition behavior. In pure methanol, PNIPAM chains existed as extended coils; in the range of volume fraction of methanol, $\varphi_{methanol}$, between 0.6 and 0.7, PNIPAM chain partially collapse into crumpled globules. In the range of $\varphi_{methanol}$ ~0.3−0.6, PNIPAM chain remained in the compact globule state. Further addition of water leads to the reswelling of the globule back to the random-coil conformation. Wang et al.[29] synthesized polymer gels consisting of *N*-isopropylacrylamide (NIPAM) and 4(5)-vinylimidazole. Taking advantage of the cononsolvency behavior of PNIPAM in ethanol/water, which results in the gel collapse or reswelling in a specific range of solvent composition, they can successfully switch on or off the catalytic activities of the polymeric gel.

On the other hand, PVim is a weakly basic linear polymer and is soluble in aqueous media and in various alcohols or a mixture of them.[53] Therefore, the micellization of PNIPAM-*b*-PVim can be realized either by increasing the temperature above the phase transition temperature of PNIPAM block or changing the solvent composition of methanol/water mixture at room temperature. In both cases, hydrophobic PNIPAM-core micelles stabilized with PVim corona will form.

Figure 4 shows the temperature dependence of average hydrodynamic radius, $\langle R_h \rangle$, and scattering intensities for PNIPAM$_{44}$-*b*-PVim$_{51}$ and PNIPAM$_{44}$-*b*-PVim$_{21}$ aqueous solutions at a concentration of 5×10^{-4} g/mL. Obviously, for each block copolymer, when the temperature is lower than the LCST of PNIPAM, the block copolymer is molecularly soluble, $\langle R_h \rangle$ is typically less than 10 nm and the scattering intensity is very weak.[53] At elevated temperatures, micellization starts to take place, $\langle R_h \rangle$ and the scattering intensities increase dramatically. At even higher temperatures, $\langle R_h \rangle$ and scattering intensities keep almost constant. The critical micellization temperatures (cmts) of PNIPAM$_{44}$-*b*-PVim$_{51}$ and PNIPAM$_{44}$-*b*-PVim$_{21}$ are 36 and 34 °C, respectively, which are higher than that of PNIPAM homopolymers. This is due to that PNIPAM is now attaching with a hydrophilic PVim block.[32] The actual morphology of

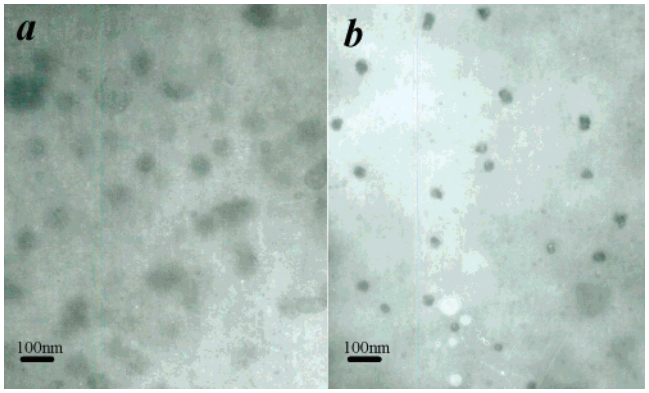

Figure 5. TEM images for (a) PNIPAM$_{44}$-*b*-PVim$_{21}$ and (b) PNIPAM$_{44}$-*b*-PVim$_{51}$ micelles in aqueous solution at 40 °C.

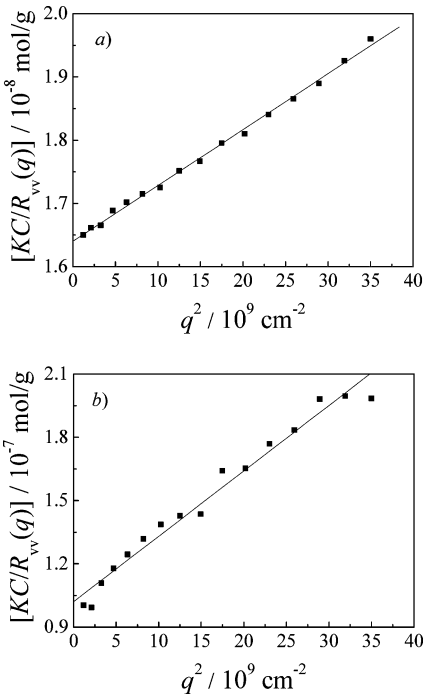

Figure 6. Scattering vector (q) dependence of Rayleigh ratio $R_{vv}(q)$ of (a) PNIPAM$_{44}$-*b*-PVim$_{21}$ and (b) PNIPAM$_{44}$-*b*-PVim$_{51}$ in aqueous solutions at 40 °C. The polymer concentration was both 5×10^{-4} g/mL.

the micellar aggregates formed at 40 °C was observed by TEM (Figure 5). It clearly revealed the presence of spherical nanoparticles of ~20−30 and 60−80 nm in diameter for PNIPAM$_{44}$-*b*-PVim$_{51}$ and PNIPAM$_{44}$-*b*-PVim$_{21}$, respectively. As TEM determined the micelle dimensions in the dry state, while dynamic LLS report the intensity-average dimensions of micelles in solution which contains the contribution from the swollen corona, it is reasonable that the micelle sizes determined by TEM were smaller than that by LLS.

Khokhlov et al.[23,31] employed imidazole-containing random copolymers of Vim and NIPAM as hydrolytic catalysts. At temperatures above the phase transition temperature, enhanced catalytic activity was observed due to the formation of globular aggregates. However, further increasing the temperatures lead to secondary aggregates, i.e., the initially formed aggregates were not stable, and reaction rate decreased correspondingly. In our case, stable micelles with hydrophobic PNIPAM core were formed even at higher temperatures due to the stabilization of the hydrophilic PVim block.

Figure 6 shows the angular dependence of the Raylaigh ratio, $R_{vv}(q)$, of micelle solutions determined by static LLS over a

Table 1. Laser Light Scattering Characterization of Micelles Formed by PNIPAM-*b*-PVim Diblock Copolymers at 40 °C and a Polymer Concentration of 5×10^{-4} g/mL

samples[a]	cmt[b] (°C)	$M_{w,micelles}$[c]	$\langle R_g \rangle$[c]/nm	$\langle R_h \rangle$/nm	μ_2/Γ^2	$\langle R_g \rangle/\langle R_h \rangle$	N_{agg}
$PNIPAM_{44}$-*b*-$PVim_{21}$	34	6.3×10^7	89	127	0.08	0.70	9100
$PNIPAM_{44}$-*b*-$PVim_{51}$	36	9.5×10^6	31	34	0.12	0.91	970

[a] The DP of each blocks were obtained from ^{1}H NMR. [b] Critical micellization temperature. [c] The accuracy of determination was ± 3%.

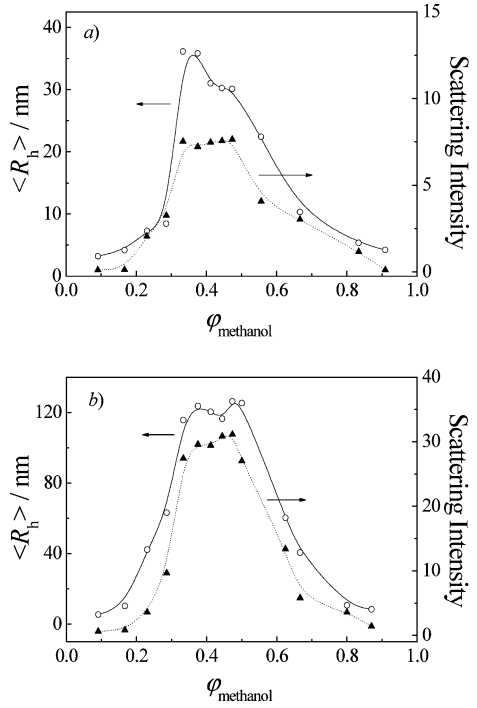

Figure 7. Average hydrodynamic radius, $\langle R_h \rangle$, and scattering intensities for (a) $PNIPAM_{44}$-*b*-$PVim_{51}$ and (b) $PNIPAM_{44}$-*b*-$PVim_{21}$ solutions as a function of the volume fraction of methanol, $\varphi_{methanol}$, in methanol/buffer (pH 7.4) mixture. The polymer concentration was 5×10^{-4} g/mL.

scattering angle range 15−90°. Table 1 summarizes the laser light scattering characterization results of micelles formed by PNIPAM-*b*-PVim diblock copolymers at 40 °C. Compared to that of $PNIPAM_{44}$-*b*-$PVim_{51}$, micelles of $PNIPAM_{44}$-*b*-$PVim_{21}$ are larger, possessing a much higher average aggregation numbers per micelles, N_{agg}. This is reasonable considering that the former has a shorter PVim length. In the catalytic studies discussed later, water/IPA mixed solvent (10% IPA) was used. Preliminary studies revealed that the presence of a small amount of IPA did not appreciably affect the thermoresponsive micellization behavior of PNIPAM-*b*-PVim.

It is well-known that a proper mixture of methanol and water is a poor solvent for PNIPAM homopolymer chains.[32] The water/methanol complexation can induce reentrant coil-to-globule-to-coil transition of individual homopolymer chains in extremely dilute solution. We then investigated the cononsolvency-induced micellization of $PNIPAM_{44}$-*b*-$PVim_{21}$ and $PNIPAM_{44}$-*b*-$PVim_{51}$ diblock copolymers in methanol/water mixed solvent with different compositions at 20 °C. Apparently, we can observe the bluish tinge at intermediate volume fractions of methanol, which is characteristic of micellar solutions. It is noteworthy that the micelles are quite stable. Figure 7 shows the variation of $\langle R_h \rangle$ and scattering intensities of block copolymer solutions as a function of the volume fraction of methanol, $\varphi_{methanol}$. In the range of $\varphi_{methanol} \sim 0.3-0.5$, $\langle R_h \rangle$ of $PNIPAM_{44}$-*b*-$PVim_{51}$ and $PNIPAM_{44}$-*b*-$PVim_{21}$ solutions exhibits a maximum, indicating that PNIPAM-core micelles were formed due to the cononsolvency of PNIPAM in this specific solvent range. $\langle R_h \rangle$ values were ∼30 and 120 nm, respectively.

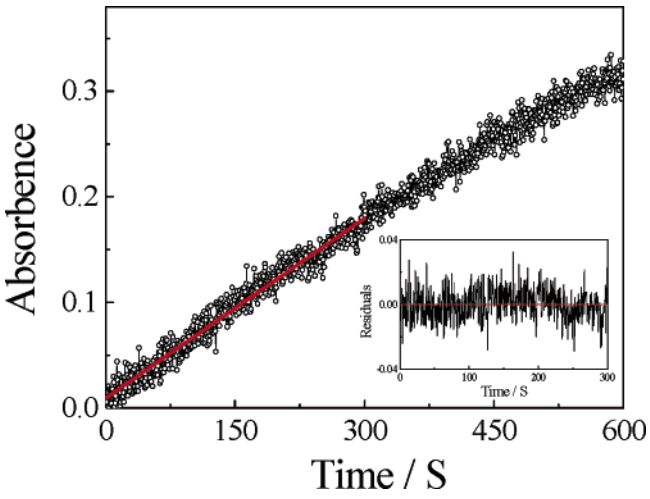

Figure 8. Typical time dependence of the solution absorbance recorded during the hydrolysis of NPA catalyzed with diblock copolymer micelles of $PNIPAM_{44}$-*b*-$PVim_{51}$ at 313 K. The wavelength was set at 402 nm. It was fitted by the linear function, $y = at + b$, within the first 300 s.

Catalytic Reaction Kinetics. In the catalytic hydrolysis experiment, we employed the stopped-flow apparatus to accurately monitor the reaction, ensuring a homogeneous mixing of the diblock copolymer with the substrate within a typical dead time of <3 ms. The hydrolysis of 4-nitrophenyl acetate results in the formation of a colored product, *p*-nitrophenol. After calibration, the change in the absorbance at 402 nm, characteristic of the ionized *p*-nitrophenol, were followed spectrophotometrically to record the reaction kinetics.

Figure 7 shows typical time dependence of absorbance recorded during the hydrolysis of NPA catalyzed with diblock copolymer micelles at 40 °C. The concentrations of Vim units and NPA were fixed at 2 mM. In the initial stage, the absorbance increased linearly with time. But after 10 min, downward curvature can be observed. The slope of the absorbance−time curve within the first 300 s was calculated and converted to the initial hydrolysis rate using a pre-established calibration curve for *p*-nitrophenol.

For the majority of temperature activated reactions, the reaction rate is an exponential function of inverse temperature, following Arrhenius-type behavior. Thus, the initial reaction rate $\sim 1/T$ curve is linear in a semilogarithmic plot. This was indeed the case when PVim homopolymer was used as the catalyst (Figure 9a). If there are some other factors affecting the reaction rate apart from temperatures, a deviation from the linear function should be observed. Using this principle, Khokhlov et al.[23] successfully confirmed that PNIPAM-*co*-PVim random copolymers exhibited enhanced reaction rate just above the critical aggregation temperature. However, in their case, at even higher temperatures, further aggregation took place and the reaction rate decreased.

Figure 9b shows the initial reaction rate of the hydrolysis of NPA catalyzed with PNIPAM-*b*-PVim diblock copolymers as a function of $1/T$. For $PNIPAM_{44}$-*b*-$PVim_{51}$, in the temperature range 20−35 °C, $\log(V) \sim T^{-1}$ plots are linear in Arrhenius

Scheme 2. Schematic Illustration of the Catalysis Mechanism Using PNIPAM-*b*-PVim Micelles as Catalytic Nanoreactors[a]

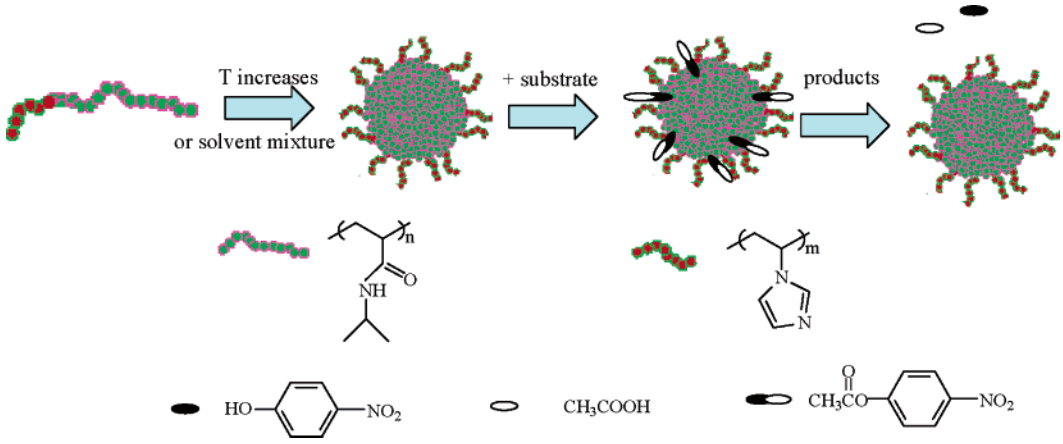

[a] The reaction rate can be well tuned by changing the temperature or solvent compositions. enhanced catalytic activities were observed when the diblock copolymers form micelles.

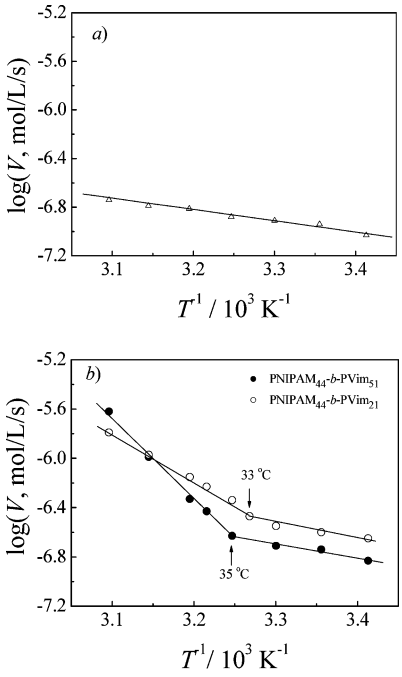

Figure 9. Initial reaction rate, *V*, of the hydrolysis of NPA catalyzed with polymeric catalysts as a function of inverse temperature: (a) PVim homopolymer; (b) PNIPAM-*b*-PVim block copolymers.

coordinates. Above 35 °C, a prominent upward curvature can be observed. For $PNIPAM_{44}$-*b*-$PVim_{21}$, the critical temperature above which enhanced reaction rates were observed decreased to ~33 °C. The inflection point is in relatively good agreement with the critical micellization temperature for both diblock copolymers (Figure 4).

Compared to PVim homopolymer, the diblock copolymers exhibit slightly higher catalytic activity, even at low temperatures. This may be due to that the DP of PVim homopolymer is larger than that of PVim blocks in the block copolymers.[25,27] From the slope of $\log(V) \sim T^{-1}$ above the critical temperature, we can also tell that $PNIPAM_{44}$-*b*-$PVim_{51}$ is more effective in the hydrolytic catalysis than that of $PNIPAM_{44}$-*b*-$PVim_{21}$. Assuming that there was no enhancement of the reaction rate due to factors other than temperature, the reaction rate can be obtained by extrapolating the linear part of $\log(V) \sim T^{-1}$ curve at low temperatures. It can be calculated that for $PNIPAM_{44}$-*b*-$PVim_{51}$ and $PNIPAM_{44}$-*b*-$PVim_{21}$, the reaction rate increased ca. 7 times and 3 times due to the micelle formation at 50 °C, respectively.

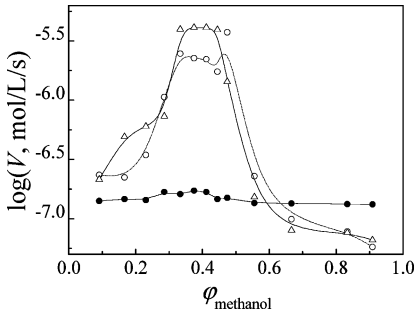

Figure 10. Initial reaction rate, *V*, of the hydrolysis of NPA catalyzed with polymeric catalysts: $PNIPAM_{44}$-*b*-$PVim_{21}$ (-□-), $PNIPAM_{44}$-*b*-$PVim_{51}$ (-○-), and PVim homopolymer (-●-) as a function of the volume fraction of methanol, $\varphi_{methanol}$, in methanol/buffer (pH 7.4) mixture. The temperatures were maintained at 20 °C.

Through the above analysis, the prominent enhancement of the catalytic activities for PNIPAM-*b*-PVim block copolymers above the critical micellization temperatures is clearly evident. The hydrophobic PNIPAM core shows good affinity for the relatively hydrophobic substrate.[54] On the other hand, NPA also exhibits some surface activities, it thus tends to be adsorbed at the core/corona interface,[23,55] and the local concentration of NPA at the interface will be much larger than that in the bulk aqueous phase. NPA was then quickly catalyzed by the relatively densely packed PVim corona, releasing water-soluble products, acetic acid and *p*-nitorphenol, into the bulk solution. An overall micellar catalysis mechanism was depicted in Scheme 2. $PNIPAM_{44}$-*b*-$PVim_{51}$ forms much smaller micelles than that of $PNIPAM_{44}$-*b*-$PVim_{21}$ (Table 1, Figure 4), thus, it was reasonable to observe that the former exhibited much higher catalytic activities due to much larger core/corona interfacial area.[24]

We thus observed for the first time that double hydrophilic block copolymer micelles of PNIPAM-*b*-PVim can serve as self-catalyzing nanoreactors. Most importantly, the catalytic activities can be well-tuned with external temperatures, via controlling the presence of block copolymers as micelles or molecularly dissolved unimers.

To further corroborate the above points and exclude the temperature effects, we examined the catalytic effects of PNIPAM-*b*-PVim micelles in the methanol/water mixed solvent at a constant temperature. Figure 10 shows initial hydrolysis rates as a function of the volume fraction of methanol, $\varphi_{methanol}$. The rate of catalysis by PVim homopolymer varied smoothly with solvent composition and did not change considerably in the whole range. In contrast, for the PNIPAM-*b*-PVim dibilock

copolymers, the catalytic activity evolved discontinuously as a function of the solvent composition and exhibited a maximum in the range of $\varphi_{methanol} \sim 0.3-0.5$, corresponding to the solvent range where cononsolvency-induced micellization took place (Figure 7). The above observations again confirmed the "micellar catalysis" mechanism as shown in Scheme 1.

Conclusions

Double hydrophilic block copolymers, poly(*N*-isopropylacrylamide)-*b*-poly(*N*-vinylimidazole) (PNIPAM-*b*-PVim), were successfully prepared with good control via the RAFT/MADIX technique. This represents the first preparation of well-defined block copolymers based on PVim, which is well-known to be able to catalyze esterolysis reactions. The imidazole-containing diblock copolymers molecularly dissolve at low temperatures in water, but at elevated temperatures above the phase transition temperature of PNIPAM block or in a proper mixture of methanol/water, PNIPAM block became hydrophobic and stable micelles formed with a dense core consisting of hydrophobic PNIPAM block and a polar shell formed by PVim block.

The catalytic activities of $PNIPAM_{44}$-*b*-$PVim_{51}$ and $PNIPAM_{44}$-*b*-$PVim_{21}$ toward the hydrolysis of *p*-nitrophenyl acetate (NPA) at different temperatures or methanol/water compositions were then determined and compared to that of the PVim homopolymer. Although the $\log(V) \sim T^{-1}$ (Arrhenius) plot, where V is the initial rate of hydrolysis and T the temperature, for PVim homopolymer was linear, the plot for the PVim-based diblock copolymers exhibited a pronounced upward curvature at temperatures above the LCST of the PNIPAM block, in which range PNIPAM-core micelles were formed.

Consistently, in methanol/water mixture, the reaction rates remained almost constant for PVim homopolymer catalysts, while for the PNIPAM-*b*-PVim dibilock copolymers, the catalytic activity evolved discontinuously as a function of the solvent composition and exhibited a maximum in the range of $\varphi_{methanol} \sim 0.3-0.5$, corresponding to the solvent range where cononsolvency-induced micellization took place. We thus observed for the first time that double hydrophilic block copolymer micelles can serve as self-catalyzing nanoreactors. Most importantly, the catalytic activities can be well-tuned with external temperatures or solvent compositions. A possible mechanism was tentatively proposed.

Acknowledgment. This work was financially supported by an Outstanding Youth Fund (50425310) and research grants (20534020 and 20674079) from the National Natural Scientific Foundation of China (NNSFC), the "Bai Ren" Project of the Chinese Academy of Sciences, and the Program for Changjiang Scholars and Innovative Research Team in University (PCSIRT).

References and Notes

(1) Hamley, I. W. *The Physics of Block Copolymers*; Oxford University Press: Oxford, U.K., 1998.
(2) Fustin, C. A.; Abetz, V.; Gohy, J. F. *Eur. Phys. J. E* **2005**, *16*, 291−302.
(3) Gohy, J. F. *Adv. Polym. Sci.* **2005**, *190*, 65−136.
(4) Hadjichristidis, N.; Iatrou, H.; Pitsikalis, M.; Pispas, S.; Avgeropoulos, A. *Prog. Polym. Sci.* **2005**, *30*, 725−782.
(5) Riess, G. *Prog. Polym. Sci.* **2003**, *28*, 1107−1170.
(6) Rodriguez-Hernandez, J.; Checot, F.; Gnanou, Y.; Lecommandoux, S. *Prog. Polym. Sci.* **2005**, *30*, 691−724.
(7) Colfen, H. *Macromol. Rapid Commun.* **2001**, *22*, 219−252.
(8) Rodriguez-Hernandez, J.; Lecommandoux, S. *J. Am. Chem. Soc.* **2005**, *127*, 2026−2027.
(9) Arotcarena, M.; Heise, B.; Ishaya, S.; Laschewsky, A. *J. Am. Chem. Soc.* **2002**, *124*, 3787−3793.
(10) Virtanen, J.; Arotcarena, M.; Heise, B.; Ishaya, S.; Laschewsky, A.; Tenhu, H. *Langmuir* **2002**, *18*, 5360−5365.
(11) Andre, X.; Zhang, M. F.; Muller, A. H. E. *Macromol. Rapid Commun.* **2005**, *26*, 558−563.
(12) Alarcon, C. D. H.; Pennadam, S.; Alexander, C. *Chem. Soc. Rev.* **2005**, *34*, 276−285.
(13) Butun, V.; Liu, S.; Weaver, J. V. M.; Bories-Azeau, X.; Cai, Y.; Armes, S. P. *React. Funct. Polym.* **2006**, *66*, 157−165.
(14) Liu, S. Y.; Armes, S. P. *Angew. Chem., Int. Ed.* **2002**, *41*, 1413−1416.
(15) Bo, Q.; Zhao, Y. *J. Polym. Sci., Part A: Polym. Chem.* **2006**, *44*, 1734−1744.
(16) Li, Y. T.; Armes, S. P.; Jin, X. P.; Zhu, S. P. *Macromolecules* **2003**, *36*, 8268−8275.
(17) Ma, Y. H.; Tang, Y. Q.; Billingham, N. C.; Armes, S. P.; Lewis, A. L.; Lloyd, A. W.; Salvage, J. P. *Macromolecules* **2003**, *36*, 3475−3484.
(18) Mountrichas, G.; Pispas, S. *Macromolecules* **2006**, *39*, 4767−4774.
(19) Pispas, S. *J. Polym. Sci., Part A: Polym. Chem.* **2006**, *44*, 606−613.
(20) Vamvakaki, M.; Palioura, D.; Spyros, A.; Armes, S. P.; Anastasiadis, S. H. *Macromolecules* **2006**, *39*, 5106−5112.
(21) Vandermeulen, G. W. M.; Tziatzios, C.; Duncan, R.; Klok, H. A. *Macromolecules* **2005**, *38*, 761−769.
(22) Zhang, W. Q.; Shi, L. Q.; Ma, R. J.; An, Y. L.; Xu, Y. L.; Wu, K. *Macromolecules* **2005**, *38*, 8850−8852.
(23) Okhapkin, I. M.; Bronstein, L. M.; Makhaeva, E. E.; Matveeva, V. G.; Sulman, E. M.; Sulman, M. G.; Khokhlov, A. R. *Macromolecules* **2004**, *37*, 7879−7883.
(24) Okhapkin, I. M.; Makhaeva, E. E.; Khokhlov, A. R. *Adv. Polym. Sci.* **2006**, *195*, 177−210.
(25) Overberger, C. G.; Okamoto, Y. *Macromolecules* **1972**, *5*, 363−368.
(26) Overberger, C. G. T.; Pierre, S.; Vorchheimer, N.; Yaroslavsky, S. *J. Am. Chem. Soc.* **1963**, *85*, 3513−3515.
(27) Simmons, M. R.; Patrickios, C. S. *J. Polym. Sci., Part A: Polym. Chem.* **1999**, *37*, 1501−1512.
(28) Overberger, C. G.; Kawakami, Y. *J. Polym. Sci., Part A: Polym. Chem.* **1978**, *16*, 1249−1263.
(29) Wang, G. Q.; Kuroda, K.; Enoki, T.; Grosberg, A.; Masamune, S.; Oya, T.; Takeoka, Y.; Tanaka, T. *Proc. Natl. Acad. Sci. U.S.A.* **2000**, *97*, 9861−9864.
(30) Patrickios, C. S.; Simmons, M. R. *Colloids Surf. A: Physicochem. Eng. Asp.* **2000**, *167*, 61−72.
(31) Lozinsky, V. I. **2006**, *196*, 87−127.
(32) Schild, H. G. *Prog. Polym. Sci.* **1992**, *17*, 163−249.
(33) Lozinsky, V. I.; Simenel, I. A.; Kulakova, V. K.; Kurskaya, E. A.; Babushkina, T. A.; Klimova, T. P.; Burova, T. V.; Dubovik, A. S.; Grinberg, V. Y.; Galaev, I. Y.; Mattiasson, B.; Khokhlov, A. R. *Macromolecules* **2003**, *36*, 7308−7323.
(34) Dwars, T.; Paetzold, E.; Oehme, G. *Angew. Chem., Int. Ed.* **2005**, *44*, 7174−7199.
(35) Simmons, M. R.; Patrickios, C. S. *Macromolecules* **1998**, *31*, 9075−9077.
(36) Hawker, C. J.; Bosman, A. W.; Harth, E. *Chem. Rev.* **2001**, *101*, 3661−3688.
(37) Chiefari, J.; Chong, Y. K.; Ercole, F.; Krstina, J.; Jeffery, J.; Le, T. P. T.; Mayadunne, R. T. A.; Meijs, G. F.; Moad, C. L.; Moad, G.; Rizzardo, E.; Thang, S. H. *Macromolecules* **1998**, *31*, 5559−5562.
(38) Chong, Y. K.; Le, T. P. T.; Moad, G.; Rizzardo, E.; Thang, S. H. *Macromolecules* **1999**, *32*, 2071−2074.
(39) Wang, J. S.; Matyjaszewski, K. *Macromolecules* **1995**, *28*, 7901−7910.
(40) Matyjaszewski, K.; Xia, J. H. *Chem. Rev.* **2001**, *101*, 2921−2990.
(41) Perrier, S.; Takolpuckdee, P. *J. Polym. Sci., Part A: Polym. Chem.* **2005**, *43*, 5347−5393.
(42) Wan, D.; Satoh, K.; Kamigaito, M.; Okamoto, Y. *Macromolecules* **2005**, *38*, 10397−10405.
(43) Shi, L.; Chapman, T. M.; Beckman, E. J. *Macromolecules* **2003**, *36*, 2563−2567.
(44) Charmot, D.; Corpart, P.; Adam, H.; Zard, S. Z.; Biadatti, T.; Bouhadir, G. *Macromol. Symp.* **2000**, *150*, 23−32.
(45) Taton, D.; Wilczewska, A. Z.; Destarac, M. *Macromol. Rapid Commun.* **2001**, *22*, 1479.
(46) Kulkarni, S.; Schilli, C.; Grin, B.; Muller, A. H. E.; Hoffman, A. S.; Stayton, P. S. *Biomacromolecules* **2006**, *7*, 2736−2741.
(47) Qiu, X. P.; Winnik, F. M. *Macromolecules* **2007**, *40*, 872−878.
(48) Schild, H. G.; Muthukumar, M.; Tirrell, D. A. *Macromolecules* **1991**, *24*, 948−952.
(49) Winnik, F. M.; Ottaviani, M. F.; Bossmann, S. H.; Garciagaribay, M.; Turro, N. J. *Macromolecules* **1992**, *25*, 6007−6017.
(50) Winnik, F. M.; Ottaviani, M. F.; Bossmann, S. H.; Pan, W. S.; Garciagaribay, M.; Turro, N. J. *Macromolecules* **1993**, *26*, 4577−4585.
(51) Costa, R. O. R.; Freitas, R. F. S. *Polymer* **2002**, *43*, 5879−5885.

(52) Zhang, G. Z.; Wu, C. *J. Am. Chem. Soc.* **2001**, *123*, 1376−1380.
(53) Savin, G.; Burchard, W.; Luca, C.; Beldie, C. *Macromolecules* **2004**, *37*, 6565−6575.
(54) Kanazawa, H.; Yamamoto, K.; Matsushima, Y.; Takai, N.; Kikuchi, A.; Sakurai, Y.; Okano, T. *Anal. Chem.* **1996**, *68*, 100−105.
(55) Vasilevskaya, V. V.; Aerov, A. A.; Khokhlov, A. R. *Dokl. Phys. Chem.* **2004**, *398*, 1.

MA070550I